

Supplemental Material

ICAM-1 engagement modulates sphingomyelinase and ceramide, supporting uptake of drug carriers by the vascular endothelium

Daniel Serrano¹, Tridib Bhowmick², Rishi Chadha², Carmen Garnacho², and Silvia Muro^{2,3}

¹Department of Cell Biology & Molecular Genetics and Biological Sciences Graduate Program; ²Institute for Biosciences & Biotechnology Research and ³Fischell Department of Bioengineering, University of Maryland, College Park, MD

Corresponding author:

Silvia Muro

5115 Plant Sciences Building, University of Maryland, College Park, MD 20742

muro@umd.edu

Phone/Fax: 301-405-4777 / 301-314-9075

Running title: Role of sphingomyelinase in endocytosis via ICAM-1

Extended Methods

Antibodies and reagents

Monoclonal antibodies to the extracellular domain of human or mouse ICAM-1 were R6.5 and phycoerythrin-conjugated LB-2 (Santa Cruz Biotechnology, Santa Cruz, CA), or YN1, respectively¹. Monoclonal antibodies to mouse platelet-endothelial cell adhesion molecule 1 (PECAM-1), human clathrin heavy chain, human vascular cell adhesion molecule 1 (VCAM-1), human mannose 6-phosphate receptor (M6PR), or ceramide were from BD Biosciences (Franklin Lakes, NJ), EMD Chemicals (Gibbstown, NJ), Millipore (Billerica, MA), or Sigma-Aldrich. (Saint Louis, MO). Polyclonal antibodies to human acid sphingomyelinase (ASM), Na⁺/H⁺ exchanger protein 1 (NHE1) or ganglioside GM1 were from Santa Cruz Biotechnology or EMD Chemicals. Secondary antibodies were from Jackson Immunoresearch (West Grove, PA). Polystyrene-latex beads were from Polysciences (Warrington, PA). BODIPY® FL C12-sphingomyelin and Texas Red-labeled phalloidin were from Molecular Probes, Inc. (Eugene, OR). Human recombinant ASM was provided by Dr. Edward Schuchman (Mount Sinai School of Medicine, New York, NY) and neutral SM was from Sigma-Aldrich. All other reagents were from Sigma-Aldrich.

Cell cultures

Human umbilical vein endothelial cells (HUVECs) purchased from Lonza Walkersville (Walkersville, MD) were cultured in M-199 medium supplemented as described². Mouse lung endothelial cells (MLECs) were isolated from wild-type C57BL/6 (The Jackson Laboratory, Bar Harbor, ME) or ASM^{-/-} mice³ (kindly provided by Dr. Edward Schuchman, Mount Sinai School of Medicine, New York, NY). Isolation of lungs from mice was done after anesthesia by intraperitoneal injection with 100 mg/kg body-weight ketamine and 10 mg/kg body-weight xylazine, and adjusted to IACUC regulations. Mouse lungs were cut into 1-2 mm fragments, followed by digestion overnight at 4°C in 1 mg/mL collagenase and filtration through a 40 µm nylon mesh⁴. Cells were isolated by incubation with anti-PECAM Mec13.3-coated Dynabeads® (Invitrogen Corporation, Carlsbad, CA) for 30 min at 4°C, and cultured in supplemented DMEM⁴. For experiments, ECs were seeded on 1%-gelatin-coated glass coverslips. Cells

were treated for 16 h with 10 ng/mL TNF α (BD Biosciences, Franklin Lakes, NJ) to induce endothelial activation and up-regulation of ICAM-1 expression².

Preparation of model polymer carriers targeted to cell surface markers

Model polymer carriers targeted to ICAM-1 to induce CAM-mediated endocytosis, or to VCAM-1 or M6PR used as controls, were prepared by adsorbing the corresponding antibodies on the surface of 100 nm- or 4.5 μ m-diameter polystyrene particles (anti-ICAM, anti-VCAM, or anti-M6PR carriers), as described^{2, 5-7}. Non-coated antibodies were separated by centrifugation and the resulting coated carriers were resuspended in phosphate buffered saline (PBS) containing 1% bovine serum albumin, and sonicated at low power for 20 s to avoid aggregation. As measured in parallel using ¹²⁵Iodinated antibody counterparts, the antibody surface density on 4.5 μ m-diameter carriers was \sim 5,000 antibody molecules/ μ m² (\sim 320,000 antibody molecules/carrier), while the antibody density on 100 nm-diameter carriers (which exhibited a final diameter of \sim 180 nm after coating, determined by dynamic light scattering) was \sim 7,000 antibody molecules/ μ m² (\sim 250 antibody molecules/carrier).

Alternatively, for experiments to rescue CAM-endocytosis by coating recombinant ASM on carrier articles, 4.5 μ m carriers were prepared using a 50:50 mass-ratio mix of anti-ICAM and either control IgG or ASM, rendering \sim 2,500 anti-ICAM molecules/ μ m².

Enrichment of lipids at sites of ICAM-1 engagement on the endothelial plasmalemma

Anti-ICAM carriers (4.5 μ m in diameter) were incubated for 15 min at 37°C with control HUVECs or HUVECs treated with 5 mM methyl- β -cyclodextrin (Cdx, a cholesterol chelator), 20 μ M 5-(N-ethyl-N-isopropyl)amiloride (EIPA, which inhibits NHE1 involved in CAM-mediated endocytosis), 50 μ M imipramine (an inhibitor of ASM), or a mix of 50 μ M imipramine and 500 mU/mL neutral SM (to inhibit endogenous ASM while rescuing this enzyme activity). Carriers that were not firmly bound to HUVECs were washed, and cells were fixed with cold 2% paraformaldehyde. Binding and/or engulfment of anti-ICAM carriers by ECs were verified by scanning electron microscopy (SEM). In parallel, cholesterol was stained using 50 μ g/mL filipin and sphingomyelin was visualized by incubating HUVECs with 0.2 μ g/mL

BODIPY®-sphingomyelin for 16 h prior to experiments⁵. Ganglioside GM1 and ceramide were detected by immunostaining.

For analysis, carriers were first located using phase-contrast microscopy (Olympus IX81, Olympus, Inc., Center Valley, PA) with a 40x oil immersion objective (UPlanApo, Olympus, Inc., Center Valley, PA). Fluorescence micrographs at the identified positions were then obtained in the z-axis every 0.5 μm , using an ORCA-ER camera (Hamamatsu Corporation, Bridgewater, NJ) and SlideBook™ 4.2 software (Intelligent Imaging Innovations, Denver, CO), and images were analyzed using Image-Pro 6.3 (Media Cybernetics, Bethesda, MD). Enrichment of lipid molecules in areas of the EC plasmalemma where carriers were bound was visualized using pseudocolored fluorescence-intensity surface plots, which were obtained at the focal plane of the plasmalemma surface versus the carrier mid cross-section. The mid cross-section of carriers is raised $\sim 2 \mu\text{m}$ above the plasmalemma level; hence, enrichment of cellular molecules at this focal plane shows EC membrane actively engulfing said carriers. For semi-quantitative analysis of these experiments, fluorescence intensity profiles were averaged from ≥ 32 carriers and enrichment of a particular lipid was calculated as fold increase (Δ) in the average intensity at the mid cross-section region of engulfed carriers divided by the average intensity of $\sim 2 \mu\text{m}$ surrounding areas where the plasmalemma is not raised engulfing carriers (“background”).

Recruitment of proteins at sites of ICAM-1 engagement on the endothelial plasmalemma

Anti-ICAM, anti-VCAM, or anti-M6PR carriers (4.5 μm in diameter) were incubated for 15 min or 30 min at 37°C with control HUVECs or HUVECs treated with 5 mM Cdx (to chelate cholesterol), 50 μM imipramine (to inhibit ASM), a mix containing 50 μM imipramine and 500 mU/mL neutral SM (to inhibit endogenous ASM while rescuing this enzyme activity), 3 mM amiloride or 20 μM EIPA (to inhibit NHE1-dependent CAM-mediated endocytosis), 0.5 μM wortmannin (to inhibit PI3 kinase), or 10 μM 1-(5-isoquinolinylnsulfonyl)-2-methyl-piperzine (H-7, to inhibit PKC). Anti-ICAM on the surface of carriers was detected by immunofluorescence using a secondary antibody. ICAM-1, VCAM-1, or M6PR were immunostained using antibodies that recognize extracellular domains of these antigens and do not require cell permeabilization. Immunostainings of ASM, NHE1, or clathrin heavy chain were performed after permeabilization with cold 0.2% Triton X-100.

For visualization and semi-quantitative analysis of the enrichment of molecules at sites of carrier binding, we used the protocol described above. In addition, the intracellular distribution of ASM was assessed by computing the total number of ASM-positive vesicles (~100-300 nm fluorescent objects) and those located within 5 μm distance around the nucleus (perinuclear). Peripheral intracellular ASM was calculated as the number of total – perinuclear ASM-positive vesicles.

Co-precipitation of ASM, α -actinin, and moesin with ICAM-1 upon ICAM-1 crosslinking was assessed by incubating HUVECs with anti-ICAM Protein A-coated magnetic Dynabeads® (Invitrogen, Grand Island, NY) for 15 min at 37°C as described⁸, followed by isolation of the magnetic beads bound to cells. Bead-bound proteins were then eluted and separated using SDS polyacrylamide gel electrophoresis. Coomassie-stained protein bands at the expected molecular weight of ASM, α -actinin, moesin, and ICAM-1 were excised from the gel, digested with trypsin, and analyzed by liquid chromatography/mass spectrometry for protein identification using Scaffold™ (Proteome Software Inc., Portland, OR).

Actin remodeling and CAM-mediated endocytosis of anti-ICAM carriers

For visualization of filamentous actin (F-actin), TNF α -activated HUVECs were incubated with 4.5 μm anti-ICAM carriers for 15 min at 37°C, followed by washing, fixation, permeabilization, and fluorescent labeling of F-actin using Texas Red-conjugated phalloidin.

For experiments of endocytosis in cell culture, TNF α -activated HUVECs, wild-type MLECs or ASM^{-/-} MLECs were incubated at 37°C with 4.5 μm anti-ICAM carriers for 30 min to allow carrier binding, followed by washing non-bound carriers and incubation at 37°C for 1 h to allow full endocytosis. Inhibition experiments were performed in the presence of 3 mM amiloride, 50 μM imipramine, 0.5 μM wortmannin, 10 μM H-7, or in Na⁺-depleted ionic solution (138 mM choline chloride, 5.4 mM KCl, 1 mM CaCl₂, 1 mM MgCl₂). Endocytosis of carriers displaying 50% anti-ICAM surface-density was also tested, as well as the effect of co-coating carriers with both anti-ICAM and with recombinant ASM, to rescue this activity in the presence of inhibitors. After cell fixation with cold 2% paraformaldehyde, samples were stained using Texas Red-labeled goat anti-mouse IgG, which binds to the anti-ICAM coat on non-internalized carriers. We have previously shown that, due to absence of a permeabilization step, this secondary antibody does

not gain access to internalized carriers². Uptake can then be determined by fluorescence microscopy using Image-Pro 6.3 by counting total carriers (phase contrast) and surface-bound Texas Red-fluorescent carriers^{2, 5}.

For *in vivo* experiments, C57BL/6, caveolin-1^{-/-} (Jackson Laboratory, Bar Harbor, ME) or ASM^{-/-} mice (provided by Dr. Edward Schuchman, Mount Sinai School of Medicine, New York, NY) were anesthetized by intraperitoneal injection with 100 mg/kg body-weight ketamine and 10 mg/kg body-weight xylazine, and then were injected intravenously with ~180 nm anti-ICAM carriers (instead of 4.5 μ m carriers that can cause capillary embolization due to their size). Endocytosis of anti-ICAM carriers by ECs was assessed in the lungs because this organ represents a first-pass area for materials injected intravenously, it receives the entire cardiac input, and its endothelium expresses relative high levels of ICAM-1, altogether providing good endothelial binding of anti-ICAM carriers, as previously shown⁵⁻⁷. Mice were subjected to intracardial perfusion with saline 3 h after carrier injection to remove circulating carriers and carriers loosely bound to the vasculature. Lungs were then isolated, fixed in 2.5% glutaraldehyde and 0.1 M sodium cacodylate buffer, and processed into 80-90 nm-thin resin-embedded sections for transmission electron microscopy⁵. Endocytosis of anti-ICAM carriers by pulmonary ECs was semi-quantitatively assessed as the number of internalized carriers per field, as previously described⁹. Animal studies adjusted to IACUC regulations.

Statistics

Data are means \pm standard error of the mean (s.e.m.). Statistical significance was determined by Student's *t*-test.

References

1. Hsu J, Serrano D, Bhowmick T, Kumar K, Shen Y, Kuo YC, Garnacho C, Muro S. Enhanced endothelial delivery and biochemical effects of alpha-galactosidase by ICAM-1-targeted nanocarriers for Fabry disease. *Journal of Controlled Release*. 2011;149:323-331.
2. Muro S, Wiewrodt R, Thomas A, Koniaris L, Albelda SM, Muzykantov VR, Koval M. A novel endocytic pathway induced by clustering endothelial ICAM-1 or PECAM-1. *J Cell Sci*. 2003;116:1599-1609.
3. Horinouchi K, Erlich S, Perl DP, Ferlinz K, Bisgaier CL, Sandhoff K, Desnick RJ, Stewart CL, Schuchman EH. Acid sphingomyelinase deficient mice: a model of types A and B Niemann-Pick disease. *Nat Genet*. 1995;10:288-293.
4. Dong QG, Bernasconi S, Lostaglio S, De Calmanovici RW, Martin-Padura I, Breviario F, Garlanda C, Ramponi S, Mantovani A, Vecchi A. A general strategy for isolation of endothelial cells from murine tissues. Characterization of two endothelial cell lines from the murine lung and subcutaneous sponge implants. *Arteriosclerosis, Thrombosis, and Vascular Biology*. 1997;17:1599-1604.
5. Muro S, Garnacho C, Champion JA, Leferovich J, Gajewski C, Schuchman EH, Mitragotri S, Muzykantov VR. Control of endothelial targeting and intracellular delivery of therapeutic enzymes by modulating the size and shape of ICAM-1-targeted carriers. *Mol Ther*. 2008;16:1450-1458.
6. Calderon AJ, Bhowmick T, Leferovich J, Burman B, Pichette B, Muzykantov V, Eckmann DM, Muro S. Optimizing endothelial targeting by modulating the antibody density and particle concentration of anti-ICAM coated carriers. *J Control Release*. 2011;150:37-44.
7. Muro S, Dziubla T, Qiu W, Leferovich J, Cui X, Berk E, Muzykantov VR. Endothelial targeting of high-affinity multivalent polymer nanocarriers directed to intercellular adhesion molecule 1. *J Pharmacol Exp Ther*. 2006;317:1161-1169.
8. Muro S, Mateescu M, Gajewski C, Robinson M, Muzykantov VR, Koval M. Control of intracellular trafficking of ICAM-1-targeted nanocarriers by endothelial Na⁺/H⁺ exchanger proteins. *Am J Physiol Lung Cell Mol Physiol*. 2006;290:L809-817.
9. Bhowmick T, Berk E, Cui X, Muzykantov VR, Muro S. Effect of flow on endothelial endocytosis of nanocarriers targeted to ICAM-1. *J Control Release*. 2011.

Supplemental Data

Table I. Molecular components associated with CAM-mediated endocytosis induced by anti-ICAM carriers.

Molecule	Abbreviation	Roles	Inhibitors	Reference
Intercellular adhesion molecule 1	ICAM-1	Co-receptor of leukocyte β_2 integrins targeted by anti-ICAM carriers used for endothelial drug delivery	-	1, 2, 3, 6
Na ⁺ /H ⁺ exchanger 1	NHE1	H ⁺ efflux and Na ⁺ influx; crosslink to the actin cytoskeleton; interacts with ICAM-1 upon binding of anti-ICAM carriers	Amiloride and its derivative EIPA	21, 22, 45, 46
Acid sphingomyelinase	ASM	Hydrolyzes sphingomyelin into ceramide	Imipramine	31, 36, 39, 49
Cholesterol	-	Regulates lateral diffusion of molecules in the plasmalemma; rich in specialized membrane lipid domains	Chelated by cyclodextrin (Cdx)	-
Sphingomyelin	SM	Sphingolipid abundant in specialized membrane lipid domains; serves as a substrate for sphingomyelinases	-	33, 38
Ceramide	-	Sphingolipid that facilitates formation of large membrane domains, vesicles, and cytoskeletal rearrangement	-	32, 33, 34, 38
Dynamin	-	Large GTPase involved in vesicular scission	Dominant negative dynamin	6
Protein kinase C	PKC	Signaling molecule; acts upstream of CAM-mediated actin remodeling	BIM-1, H-7	6
Src kinase	-	Signaling molecule; acts upstream of CAM-mediated actin remodeling	Radicicol	6
Rho-dendent kinase	ROCK	Signaling molecule; acts upstream of CAM-mediated actin remodeling	Y27632	6
Filamentous actin	F-actin	Forms stress fibers associated to uptake of ICAM-1-targeted carriers	Depolymerized by latrunculin A	6, 21

Table II. Liquid chromatography/mass spectrometry analysis of endothelial proteins immunoprecipitated with anti-ICAM carriers.

Protein	Protein identification probability	Percent of total spectra*	Number of assigned spectra
ICAM-1	100%	2.1%	11
α -actinin	100%	2.5%	13
Moesin	100%	1.1%	6
ASM	-	Not observed	Not observed

* Total spectra include trypsin peptides and non-peptide charged molecule contaminants

Analysis used an identification filter of: Minimum 2 peptides, with 95% minimum peptide identification probability

Video I. Engulfment of anti-ICAM carriers by ICAM-1-rich areas of the endothelial plasmalemma.

Activated HUVECs were incubated with 4.5 μm anti-ICAM carriers for 15 min at 37°C to engage ICAM-1 on ECs, followed by washing and fixation. Fluorescence micrographs were obtained at different focal planes along the z-axis (167 nm steps), after staining anti-ICAM on the surface of carriers using a FITC-labeled secondary antibody and ICAM-1 on the EC surface using a Texas Red-labeled antibody. Frames run through the z-axis from the top of the carrier to the endothelial plasmalemma.

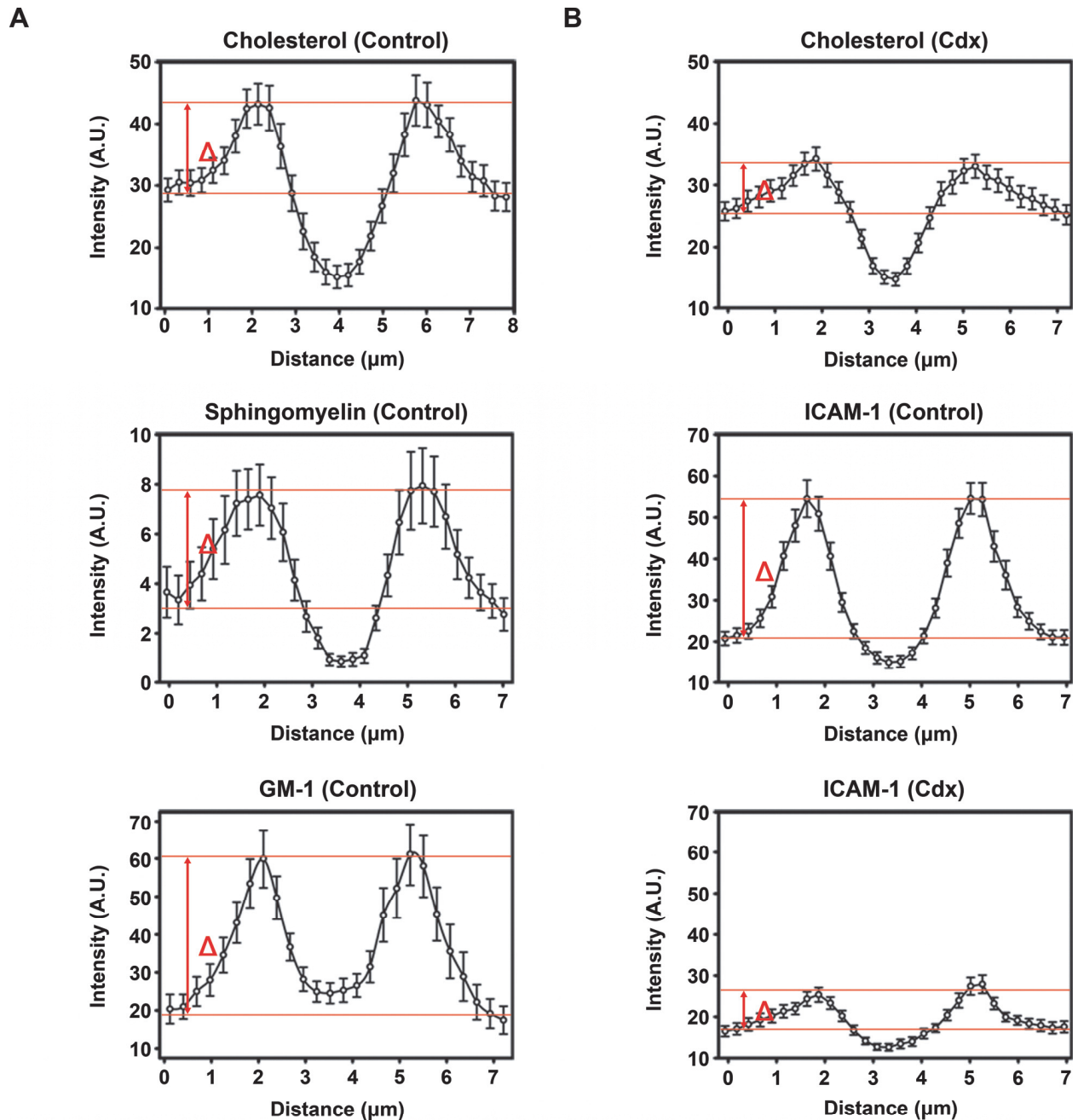


Figure I. Quantification of enrichment of lipids at sites of anti-ICAM carrier engulfment by ECs.

Activated HUVECs were incubated with 4.5 μm anti-ICAM carriers for 15 min at 37°C to engage ICAM-1 on ECs, followed by washing and fixation. (A) Cholesterol, sphingomyelin or ganglioside GM1 were stained using fluorescent blue filipin, green BODIPY-sphingomyelin, or anti-GM1 and a Texas Red-conjugated secondary antibody, respectively. (B) Effect of methyl- β -cyclodextrin (Cdx) on enrichment of

cholesterol labeled with blue filipin (upper panel) or ICAM-1 immunostained with a Texas Red-labeled antibody (middle and bottom panels) in regions of anti-ICAM-carrier binding. In all cases, graphs show fluorescence intensity plots at the mid cross-section plane of anti-ICAM carriers bound on ECs, and enrichment of molecules in these engulfment areas compared to adjacent areas of the endothelial plasmalemma (Δ , which indicates fold increase). Data represent mean and s.e.m. ($n \geq 65$ carriers).

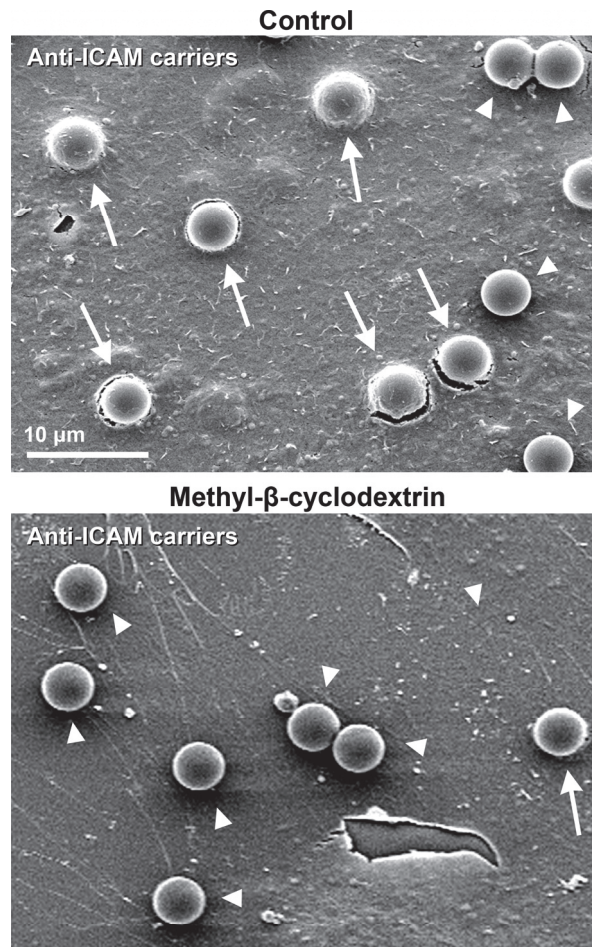


Figure II. Effect of methyl- β -cyclodextrin on engulfment of anti-ICAM carriers by ECs. Activated HUVECs were incubated with 4.5 μm anti-ICAM carriers for 15 min at 37°C to engage ICAM-1 on ECs under control conditions or in the presence of methyl- β -cyclodextrin (to remove cholesterol), following by processing for SEM visualization. Arrows indicate membrane-engulfed carriers and arrowheads indicate carriers bound to the cell surface but non-associated with engulfment structures. Scale bar = 10 μm .

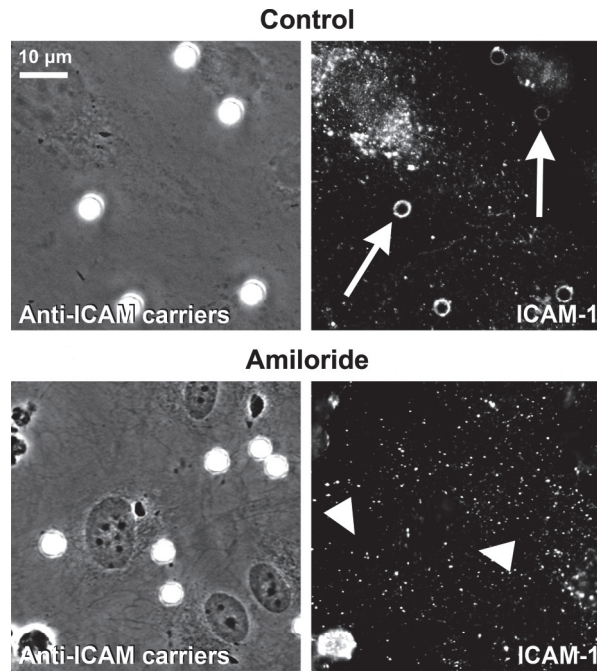


Figure III. Effect of amiloride on the engulfment of anti-ICAM carriers by ICAM-1-rich structures in ECs. Activated HUVECs were incubated for 15 min at 37°C with 4.5 µm anti-ICAM carriers to engage ICAM-1 on ECs, under control conditions or in the presence of amiloride. Cells were washed and fixed, ICAM-1 was immunostained using a Texas Red-labeled antibody, and samples were observed by phase-contrast (left panels) and fluorescence (right panels) microscopy. Presence or absence of carrier engulfment is marked with arrows or arrowheads, respectively. Scale bar = 10 µm.

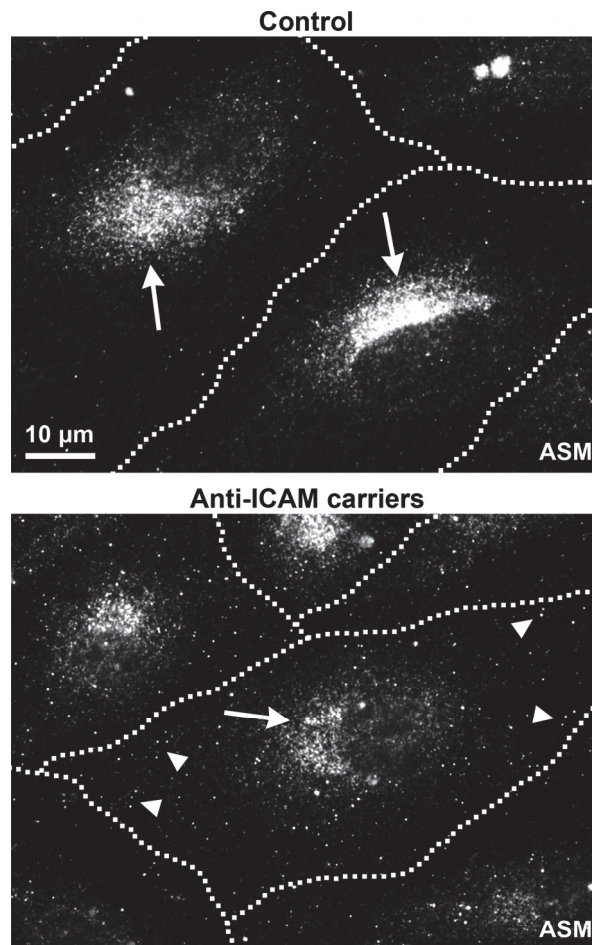


Figure IV. Redistribution of endothelial ASM upon ICAM-1 engagement by anti-ICAM carriers.

Activated HUVECs were incubated in the absence (Control) or presence of anti-ICAM carriers for 30 min at 37°C. Cells were fixed and permeabilized, and ASM was stained with a Texas Red-labeled secondary antibody. Arrowheads mark ASM at the perinuclear region of cells. Arrows mark ASM at the cell periphery. Dashed lines mark the cell borders, as observed by phase contrast. Scale bar = 10 μ m.

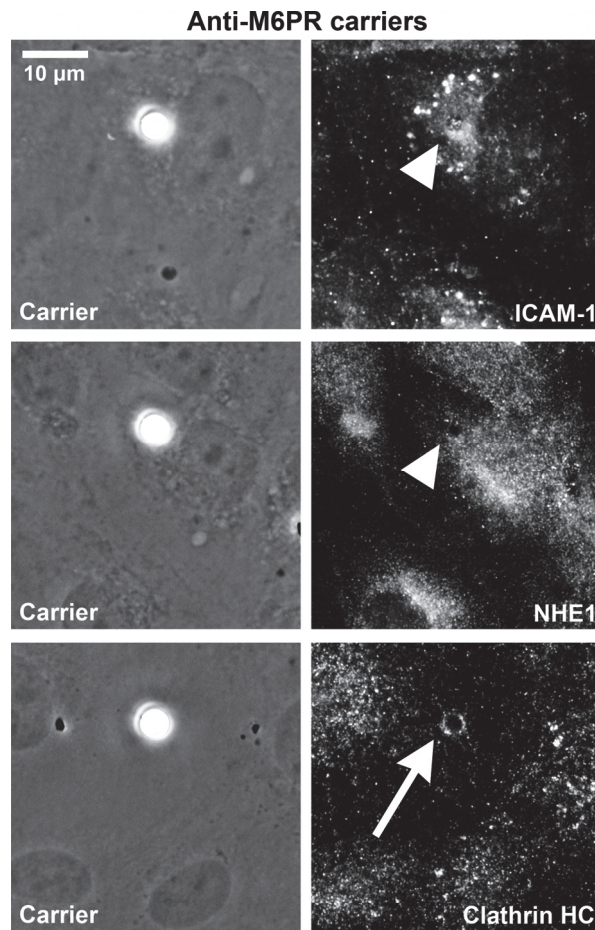


Figure V. Recruitment of molecules at sites of M6PR engagement by anti-M6PR carriers. Activated HUVECs were incubated with 4.5 μm anti-mannose-6-phosphate receptor (M6PR) carriers for 15 min at 37°C to engage M6PR on ECs, followed by washing and fixation. Phase contrast (left panels) and fluorescence micrographs (right panels) were obtained after immunostaining ICAM-1, NHE1, or clathrin heavy chain with Texas Red. Arrowheads indicate lack of enrichment of the corresponding marker around carriers. Arrows indicate enrichment of the corresponding marker around carriers. Scale bar = 10 μm .

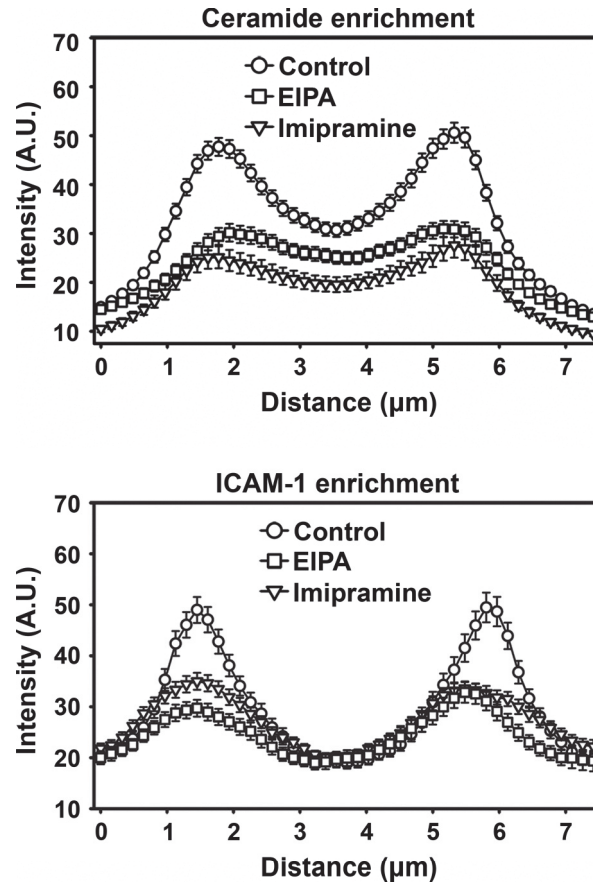


Figure VI. Quantification of ceramide enrichment and contribution of ASM and NHE1 to engulfment of anti-ICAM carriers by ECs. Activated HUVECs were incubated with 4.5 μm anti-ICAM carriers for 15 min at 37°C to engage ICAM-1 on ECs under control conditions or in the presence of EIPA (to inhibit NHE1) or imipramine (to inhibit ASM), followed by washing and fixation. Ceramide (top) or ICAM-1 (bottom) were immunostained. Graphs show fluorescence intensity plots at the mid cross-section plane of anti-ICAM carriers bound on ECs. Data represent mean and s.e.m. ($n \geq 150$ carriers).